

# Development of an Ultrasonic Clutch

Tatsuya Koyama

Keio University, 3-14-1 Hiyoshi Kohoku-ku, Yokohama, Japan, 223-8522

Kenjiro Takemura

Tokyo Institute of Technology, 4259 Nagatsuda-cho Midori-ku, Yokohama, Japan, 226-8503

Takashi Maeno

Keio University, 3-14-1 Hiyoshi Kohoku-ku, Yokohama, Japan, 223-8522

**Abstract** - In the present paper, a newly developed ultrasonic clutch is proposed. The ultrasonic clutch can solve problems of conventional passive elements, such as time delay, instability, and large size, by using unique characteristics of ultrasonic motor, as fast response, silent motion, and non-magnetic feature. It can also be designed to be smaller than conventional elements due to its simple structure. The clutch locks or releases the rotor by use of ultrasonic levitation phenomenon. First, we have designed the structure of the ultrasonic clutch using an equation of ultrasonic levitation phenomenon, results from structural analysis and finite element (FE) analysis of piezoelectric material of the vibrator. Then we have manufactured the ultrasonic clutch and have conducted a driving experiment. Finally, we have demonstrated that the maximum levitation force is around 20 N and the static friction torque of the ultrasonic clutch is up to 0.14 Nm.

## I. INTRODUCTION

For the past decade, several useful passive elements such as ER brake [1], electromagnetic powder clutch [2], and electromagnetic clutch have been developed. Although they have unique characteristics, they still have several problems in the passive elements as follows:

Using electromagnetic powder clutch, torque can be easily controlled since the current which excites the coil is in proportion to the torque. However, since it takes several tens of milliseconds to respond, it is not suitable for high-speed control.

ER brake controls torque by use of rheology characteristic of its ER fluid. Namely, the viscosity of ER fluid changes inversely in proportion to the input voltage at high speed. However, ER brake is unable to provide torque when the operator stands still because it uses the viscosity of ER fluid to control torque.

We have used an electromagnetic clutch as a passive element on our previous haptic device [3]. The weight of the electromagnetic clutch was small enough. Furthermore, the electromagnetic clutch frequently becomes unstable due to electrical noise. Hence, the problems of conventional passive elements are summarized as follows:

- (1) They are not highly responsive.
- (2) Their motions are unstable.
- (3) Their entire systems are large in size.

Therefore, it is necessary to develop a new type of passive element which solves the above-mentioned

problems.

The ultrasonic clutch solves the problems (1) and (2) by use of unique characteristics of ultrasonic motor such as fast response, silent motion and absence of electromagnetic feature. Moreover, the problem (3) is also solved since the ultrasonic clutch can be built smaller in size than the conventional ones due to simple structure of the vibrator. The ultrasonic clutch has the same unique features as ultrasonic motors; it uses an ultrasonic levitation phenomenon [4] for its operation.

## II. ULTRASONIC LEVITATION PHENOMENON

A schematic view of the vibrator is shown in Figure 1(a) and the cross sectional view of the clutch is shown in Figure 1(b). The figure does not show any other parts around the rotor and vibrator, however, a normal load is applied between rotor/vibrator by a spring to generate a static friction torque. The clutch uses the ultrasonic levitation phenomenon to levitate the rotor against the normal load to release the clutch. The clutch uses out-of-plane vibration to conduct the ultrasonic levitation phenomenon. To explain the generation of the levitation force, squeeze film theory is mainly used.

A circular object with radius  $a$  is levitating with a small gap with a vibrating plane which has uniform displacement in whole plane, where the levitation force is obtained as follows [5].

$$f_s = \int_0^a p_s \cdot 2\pi r dr = \frac{\pi a^2 \rho_0 c_0^2}{2\gamma} \quad (1)$$

where

$c_0$  = Speed of sound in reference condition [m/s]

$f_s$  = Levitation force [N]

$p_s$  = Time-average pressure of squeeze film [Pa]

$\gamma$  = Ratio of specific heats

$\rho_0$  = Density of air in reference condition [kg/m<sup>3</sup>]

Equation (1) shows the levitation force is in proportion to the contact area of rotor and vibrator. Figure 2 shows the variation of levitation force  $f_s$  against radius of the rotor  $r$  shown in Figure 1(a), where, maximum radius  $r_0$  is 14 mm which we have decided based on the size of the electromagnetic clutch used in our previous haptic device. The variation range of the inner radius  $r$  is from 0 to 13 mm.

## III. DESIGN AND IMPLEMENTATION

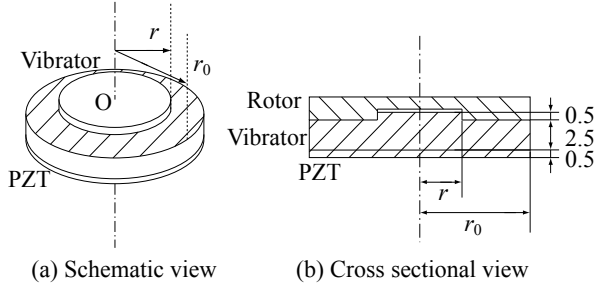


Figure 1: View of ultrasonic clutch

### Design Condition

A design condition of the ultrasonic clutch must satisfy two points as follows in order to implement it in the haptic device. First, the static friction torque of the clutch should be around 0.20 Nm. Second, both mass and size of the clutch should be less than that of the electromagnetic clutch (65g,  $\phi 28*20$  mm). These two points have been already confirmed by our previous study [3].

The static friction torque  $T$  can be calculated as follows according to Coulomb's law

$$T = Fr \quad (F = \mu N) \quad (2)$$

where  $F$ ,  $r$ ,  $\mu$  and  $N$  are static friction force, radius, static friction coefficient and normal force, respectively. The pressure between rotor and vibrator is equally distributed by using a spring to set the normal load, so the static friction torque can be obtained by integrating equation (2) as follows

$$T = 2\pi\mu P \int_{r_0}^r r^2 dr \quad (3)$$

where  $P$  is the pressure. Figure 3 shows the variation of the static friction torque against the radius. The normal loads of the curves shown in Figure 3 are 14.7 N, 19.6 N, 24.5 N and 29.5 N, respectively. The static friction torque of the clutch is approximately in inverse proportion to the contact area of rotor and vibrator because the normal load on the rotor is equally distributed. Figure 3 indicates that the static friction torque increases as radius increases. Namely, the static friction torque becomes larger as the contact area becomes smaller. On the other hand, the levitation force is in proportion to the contact area, that means, small contact area cannot generate enough levitation force. Therefore, we decided the value of radius  $r$  as 4 mm, and also designed the shape of the contact area as striped area shown in Figure 1(a). This shape enables the vibrator to levitate normal load of 29.5 N because it can generate levitation force of around 30.9 N by squeeze film effect. It indicates that the static friction torque becomes 0.20 Nm and this satisfies the design conditions mentioned above. In addition, we designed the upper surface of the vibrator convexity to keep the center of the rotor and the vibrator corresponds.

### Finite Element Analysis

This section describes the result from structural analysis and FE analysis of piezoelectric material using finite element method in order to determine the

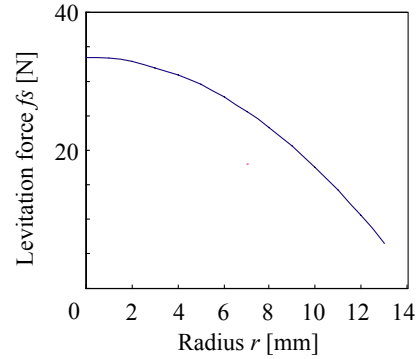


Figure 2: Radius  $r$  vs. levitation force  $f_s$

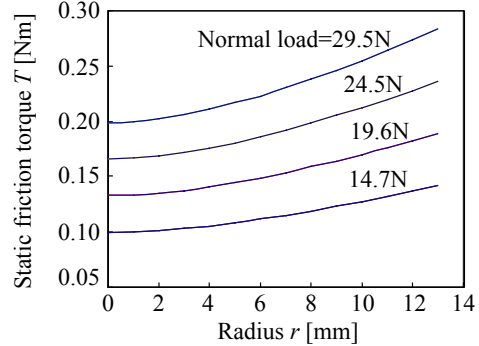


Figure 3: Radius  $r$  vs. static friction torque  $T$

characteristic of the designed vibrator.

First, the structural analysis was conducted. We made a finite element model of the vibrator. The brass, epoxy adhesive and lead zirconate titanate (PZT) were adopted in the FE model. The material properties of each material are shown in Table 1. As a result of the structural analysis using above-mentioned model, the natural frequency of the out-of-plane vibration was 21.67 kHz and the mode shape is shown in Figure 4.

Next, a FE analysis of piezoelectric material was conducted. The input voltage and the frequency to the PZT of the analysis were 5.0 V<sub>p-p</sub> and 21.65 kHz, respectively. Moreover, we defined the damping ratio  $\zeta$  as

$$\zeta = 1/2Q \quad (4)$$

where  $Q$  denotes the quality factor of the vibrator. The value of  $Q$  is around 1000 in general vibrator such as adhered brass and PZT so we used 1000 as  $Q$ . Figure 5 shows the distribution of the one side amplitude of vibration of the vibrator. As a result of the FE analysis of piezoelectric material, the amplitude of a point on the circumference of the upper surface was around 8.7  $\mu$ m. According to an experiment in previous study [5], a 25 mm-by-25 mm plate weighing 700 g have successfully levitated using vibrating plane with amplitude of 5  $\mu$ m and frequency of 20kHz. Therefore, the ultrasonic levitation phenomenon appears in case the amplitude is around 8.7  $\mu$ m.

### Implementation

The manufactured rotor and vibrator are shown in Figure 6. The rotor is also made of brass. The surface of both rotor and vibrator are coated by Nickel to protect the

Table 1: Material properties

	Brass	PZT	Epoxy adhesive
Young's modulus [GPa]	104.0	72.6	2.5
Poisson's ratio	0.33	0.31	0.40
Mass density [ $10^3 \text{kg/m}^3$ ]	8.6	7.7	2.3

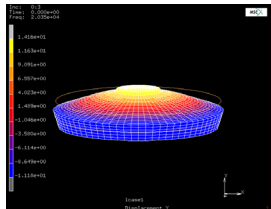


Figure 4: Mode shape of vibrator

contact surface from wearing. Mass of the vibrator is 16 g.

#### IV. DRIVING TEST

This chapter describes the result from the driving test. First, we conducted a driving test without normal load to measure the amplitude of the upper surface of the vibrator. Next, we confirmed the relationship between the amplitude and the levitation force by conducting a driving test with various normal loads.

##### Driving Test without Normal Load

We measured amplitudes of six points on the upper surface (Table 2) of the vibrator using laser doppler vibrometer (GRAPHTEC, AT7211). The input voltage and the driving frequency to the vibrator were the same as the FE analysis of piezoelectric material ( $5.0 \text{ V}_{\text{p-p}}$ ,  $21.65 \text{ kHz}$ ). The result of this measurement is shown in Figure 5 to compare with the result of the FE analysis of piezoelectric material. Although there were some errors near the center and at the edge of the surface, we can confirm that the position of the node and the mode shape are well in agreement.

##### Driving Test with Normal Load

We confirmed the relationship between the amplitude and the levitation force by conducting a driving test with various normal loads. The conditions of the normal loads and the input voltage are as follows.

First, keeping the normal load at 5 various magnitudes as shown in Figure 10, we varied the input voltage from  $20 \text{ V}_{\text{p-p}}$  to  $35 \text{ V}_{\text{p-p}}$  in increments of  $5 \text{ V}_{\text{p-p}}$ . Next, we varied the normal load as 9.8 N, 14.7 N and 19.6 N, and then measured the input voltage and the amplitude which reduced the friction torque minimally. At the same time, we chose an appropriate driving frequency which matches with the resonant frequency because the resonant frequency generally changes with the variation of the magnitude of the input voltage. The amplitude of the measurement point 6 (Table 2) was measured as typical amplitude. The levitation forces in each experiment condition were obtained by hanging some weights to the pulley. In case the clutch is locked,

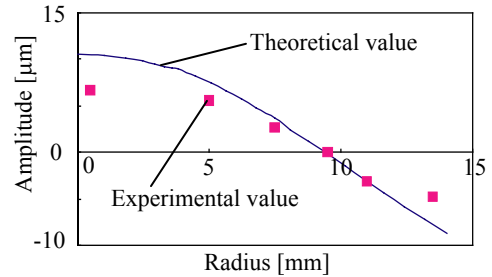


Figure 5: Radius vs. amplitude

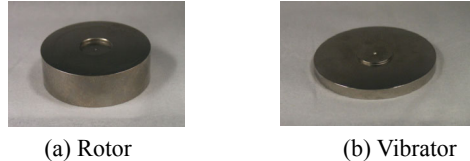


Figure 6: View of manufactured rotor and vibrator

Table 2: Locations of measurement points

Measurement point	1	2	3	4	5	6
Distance from center [mm]	0.5	5.0	7.5	9.5	11.0	13.5

the magnitude of the weight which is possible to be hanged to the pulley is in proportion to the normal load, and the magnitude of the weight is up to 2.3 kg maximally when the normal load is 29.5 N. Meanwhile, in case the clutch is released, the magnitude of the friction torque was confirmed that it reduced to less than  $1.8 \times 10^{-3} \text{ Nm}$  due to the shaft had rotated when the weights of 2 g was hanged to the pulley. The friction torque of  $1.8 \times 10^{-3} \text{ Nm}$  can be assumed as unloaded rotation compared to locked friction torque. Therefore, we defined the magnitude of the levitation force is the same as the magnitude of normal load when the friction torque became less than  $1.8 \times 10^{-3} \text{ Nm}$ . The results of these measurements are shown in Figure 9 and Figure 10.

Figure 9 shows the relationship between the change of amplitude and the levitation force. Namely, it indicates that the normal load under the curve can be levitated in case the amplitude is constant. Moreover, the magnitude of the maximum levitation force was obtained as 19.6 N when the input voltage was  $45 \text{ V}_{\text{p-p}}$  and the driving frequency was  $20.81 \text{ kHz}$  by changing the normal load. In addition, as the static friction coefficient between the rotor and the vibrator had been measured as 0.7 by the preliminary experiment, the maximum static friction torque is calculated as 0.14 Nm. Furthermore, in case we increased the magnitude of the normal load up to 29.5 N, we also confirmed that the clutch could reduce the friction torque under  $1.8 \times 10^{-3} \text{ Nm}$  with the input voltage of  $98 \text{ V}_{\text{p-p}}$ . At the same time, the amplitudes were over 17  $\mu\text{m}$ . However, we also confirmed that the PZT would crack if the amplitude increases over around 12  $\mu\text{m}$  by the preliminary experiment. So the above-mentioned results with normal loads of 24.5 N and 29.5 N are supposed to be occurred with broken PZT. Therefore, we need to redesign the shape of the vibrator to levitate the

normal load over 19.6 N safely.

Figure 10 shows the amplitude varied with input voltage under constant normal load. According to the result, the amplitude of vibration is in proportion to the input voltage. Therefore, a control of friction torque is able to be conducted by changing the input voltage under constant normal load.

As a result of the simulative calculation, the clutch generated a levitation force of around 30.9 N. However, the acquired levitation force was 19.6 N. The uneven shape of the vibrating plane of the vibrator is thought to be a main cause of the difference. Moreover, the ultrasonic levitation appears to incorporate several error factors such as surface roughness of the sliding surface and a shape of vibration.

## V. DISCUSSIONS AND FUTURE WORKS

In this paper, each driving test does not include transient measurements. Therefore, an accurate measurement of setting time of the ultrasonic levitation of the clutch is one of the future works. However, the settling time is inferred to be around several milliseconds from the characteristics of ultrasonic motors such as high speed. As a result from the driving test, we demonstrated that the steady-state levitation of the clutch is stable due to its non-magnetic feature. Meanwhile, stable static friction torque can also be generated due to normal load when the clutch is locked. Therefore, we can safely say that the clutch operates stably whether it is locked or released. A quantitative evaluation of the stability of the clutch and a comparison with the electromagnetic clutch should also be done in the future works. Although the mass of the vibrator is only 16 g, the clutch can generate static friction torque of 0.14 Nm. On the other hand, the mass of the electromagnetic clutch we used in the previous haptic device is 65 g and it generates static friction torque of 0.25 Nm. In case we implement the clutch in haptic device, the design of a unit composed of the rotor, vibrator and a shaft becomes a future work. However, we expect that the use of small conical spring washer and light weight material for the casing unit can make the entire size smaller and lighter. Therefore, we can say that the torque/inertia ratio of the developed ultrasonic clutch is much more superior to the conventional passive elements. Moreover, the ultrasonic clutch is capable of providing not only two states of lock/release but also a control of various magnitude of the friction torque, although the conventional electromagnetic clutches are unable to provide holding torque that varies continuously. Therefore, the novel clutch developed in this study can be used for high precision control device by properly controlling the driving characteristics. Furthermore, the redesign of the vibrator to generate a larger levitation force should also be done in the future works.

## VI. CONCLUSIONS

The novel ultrasonic clutch is developed in the present study. The levitation force is calculated using the equation from theories that explain the ultrasonic

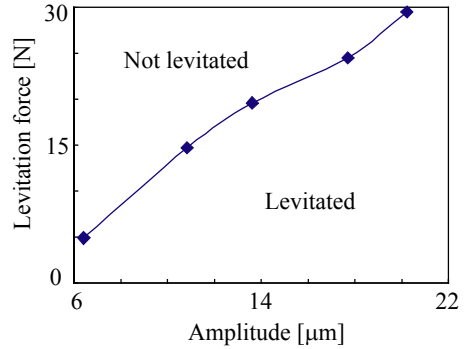


Figure 9: Amplitude vs. levitation force

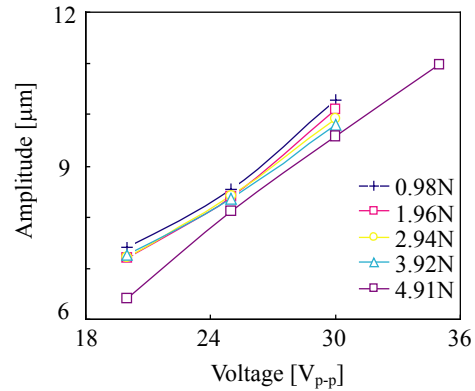


Figure 10: Amplitude vs. voltage

levitation. Furthermore, we have confirmed the natural frequency, mode shape and amplitude of the vibrator vibration by the structural analysis and FE analysis of piezoelectric material using FEM. From the driving test using the constructed ultrasonic clutch, it is demonstrated that maximum value of the levitation force is around 20 N and the static friction torque is up to 0.14 Nm.

## VII. REFERENCES

- [1] K. Fukusumi, M. Sakaguchi, J. Furusho, "Basic Study on Passive Force Display", Proceedings of the 43rd Annual Conference of the Institute of Systems, Control and Information Engineers, ISCIE, pp. 305-306, 1999
- [2] O. Saito, K. Komoriya, R. Murata, "Passive Force Display with Powder Clutch", Proc. of the 1998 JSME Conference on Robotics and Mechatronics, No. 98-4, pp. 2AII1-6, 1998(in Japanese)
- [3] T. Koyama, I. Yamano, K. Takemura and T. Maeno, "Multi-Fingered Exoskeleton Haptic Device using Passive Force Feedback for Dexterous Teleoperation", IEEE/RSJ International Conference on Intelligent Robots and System 2002, Vol. 3, pp. 2905-2910, 2002
- [4] J. J. Blech, "On Isothermal Squeeze Films", ASME Jnl. of Lubrication Technology, Vol. 105, pp. 615-620, 1983
- [5] K. Hashiba, K. Terao, T. Kunoh, "A Study on Ultrasonic Levitation", XIXth International Congress of Theoretical and Applied Mechanics, No. 1996-8, pp. 345, 1996